Proceedings of the International Gas Turbine Congress 2003 Tokyo
November 2-7, 2003

IGTC2003Tokyo TS-127

Development of turbine disk materials for aircraft engines

Satoshi TAKAHASHI[1], Sadao NISHIKIORI[1],
Masaatsu HOSOYA[2], Mikiya ARAI[2], Mitsuhiro TAKEKAWA[2] and Kazunori TAHARA[2]

[1]Research Laboratory
Ishikawajima-Harima Heavy Industries Co., Ltd.
1 Shin-Nakaharacho, Isogo, Yokohama, Kanagawa 235-8501, JAPAN
Phone: +81-45-759-2804, FAX: +81-45-759-2205, E-mail: satoshi_takahashi@ihi.co.jp
[2] Aero Engine and Space Operations
Ishikawajima-Harima Heavy Industries Co., LTD.

ABSTRACT

In this paper, recent researches about manufacturing process for turbine disk application were reported from the point of view of various properties prediction. The dual-property disk production model, microstructure and mechanical property prediction model for cast/wrought alloy were focused.

The dual-property disk has a bimodal microstructure, i.e., outer diameter region has larger grains than inner diameter region. As for the dual- property disk manufacturing process, two step solution treatment was effective. In the first step, outer diameter region of the disk was heated. During this process, primary γ' that works as an obstacle for grain growth was solved. In the second step, whole of the disk was heated and grain sizes were controlled without incipient melting. Through the estimation for the grain growth behavior, the microstructure prediction for the dual-property disk formation process was conducted.

Microstructure and mechanical property prediction model for cast/wrought U720LI were investigated. The effects of forging condition on the microstructure and the mechanism of microstructure formation were discussed. Additionally model for predicting the mechanical property of cast/wrought U720LI was also discussed. This model was estimated the effects of inhomogeneous microstructure.

INTRODUCTION

Recently, taking environmental conscious into consideration aircraft engines having high efficiency have been demanded. In order to meet these requirements, conditions of engine operation, e.g. turbine inlet gas temperature (TIT) or peripheral velocity etc., have been inclement for materials. Especially turbine disks are one of the most important parts so that many studies have been conducted.

Ni-base superalloys are applied for high-pressure turbine disks. Turbine disks are manufactured by cast and wrought process (C&W) and powder metallurgy process. These processes have both advantages and disadvantages. C&W process has been widely used. In this process, firstly, ingots are melted by double or triple melting process with the objective of eliminating inclusion and obtaining homogenized microstructure. Then ingots are cogged and die-forged to rough shape. High strength alloys don't show good forgeability because the alloys are relatively brittle in consequence of addition of various strengthening elements. When high strength disks are needed, another process, powder metallurgy (PM), has been applied. In this process, powders with many strengthening elements are used. Powder is canned and hot extruded to billets. The billets are forged to rough shape under isothermal condition. PM disks have homogeneous structure and superior strength to C&W alloys, but production costs are higher than that of C&W process. Besides, during powder manufacturing process, ceramic inclusions easily mixed in alloy powder and act as trigger of fracture.

In order to obtain high strength disks, various manufacturing processes have been widely studied. One of them is the heat treatment for dual-property disks (Hyzak et al., 1988). In this paper a microstructure prediction model for manufacturing the dual-property disk has been investigated. N18, which is a Ni-base PM alloy, is chosen as an experimental alloy.

On the other hand, mechanical properties of forged disk are strongly affected by forging conditions in case of using high performance C&W alloys thus; it is significant to choose these conditions for the purpose of obtaining homogeneous mechanical properties within a disk. Repeated trial productions combined with destructive inspection for mechanical properties can lead to high cost and low productivity. This is not acceptable. In these situations, the establishment of technology for prediction of the microstructure is demanded. In recent studies, microstructure predicting models for some Ni-base superalloys, such as Waspaloy and Inconel718 have been developed (Shen et al, 1996). But these models can only predict the microstructure. Limited research has been reported to predict mechanical properties. In order to predict the mechanical properties, the microstructure formed during forging and heat treatment has to be investigated. Therefore we have investigated the kinetics of dynamic recrystallization during the forging process and quantified the effect of microstructure on the mechanical properties for the Ni-base superalloy U720LI that is one of the high strength alloys among C&W alloys.

CURRENT OF MATERIAL DEVELOPMENT

TIT of recent engines such as V2500 or GE90 is more than 1700K and it for supersonic transport (SST) is planed to increase around 2000K. Advanced materials have been responsible to increase TIT. In general, cast/wrought alloys make their LCF lifetimes longer by refining microstructure. Thus, the powder metallurgy disk has been used to meet the increased service temperature. The alloys for powder metallurgy contain many strengthener elements and their microstructure are fine and homogeneous due to their production process. Because of these chemistry and microstructure, the alloys have superior high temperature strength to cast/wrought alloys. The points of design concept have been changing LCF properties to creep properties. This change leads to the development of powder metallurgy disks. Recently, the importance has been put on fatigue crack growth rate properties, therefore grain size are controlled to intermediate size in spite of fine grain size. At the same time, the disk that has dual -properties has been tried to produce. The outer diameter portion of

Manuscript Received on June 30, 2003

the dual-property disk has coarse grain and the inner portion has fine grain correspond to the design requirements.

HEAT-TREATMENT FOR DUAL-PROPERTY DISK

Capability of manufacturing dual-property disk is accessed. The experimental alloy is as-forged N18. N18 has good high temperature strength and fatigue crack growth resistance. The way to manufacture dual-property is as follows; firstly outside of the disk is heat–treated partially then the whole disk is heated at normal condition.

Experimental procedure

Chemistry of N18 is shown in **Table 1**. Material was melted by vacuum induction melting and atomized by gas atomization method in argon atmosphere. Then the material was hot extruded and isothermal forged. In order to make a different microstructure along disk radius, grain growth behavior during the first stage heat-treatment, i.e. partial heat-treatment applied to outer diameter, should be well understood. From this point of view, the grain growth behavior of N18 was estimated. Blocks with 10x10x10mm were cut off from the as-forged pancake and heat-treated. Heat-treatment conditions are shown in **Table 2**.

Table 1 Chemical composition of N18 (wt%)

Cr	Co	Mo	Ti	Al	Zr	Hf	B	C	Ni
11.5	15.7	6.5	4.4	4.4	0.03	0.50	.015	.013	bal.

Table 2 Heat-treatment conditions

	Solution heat treatment
C1	1433K/1, 2, 4h/O.Q.
C2	1453K/1, 2, 4, 8h/O.Q.
C3	1473K/1, 2, 4, 8h/O.Q.
C4	1493K/0.5, 1, 2/O.Q.
R1	1473K/0.5h/O.Q. ->1453K/1, 2, 4h/O.Q.

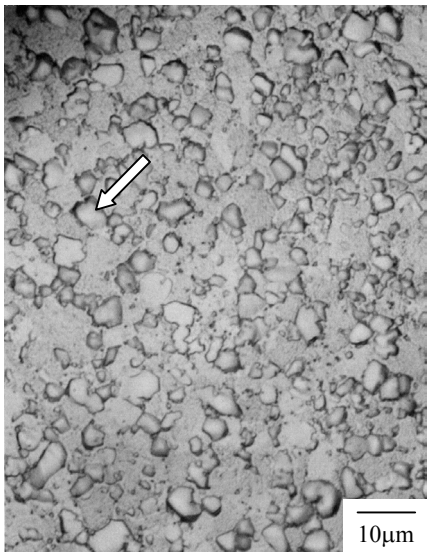

Fig.1 Microstructure of as-forged N18

The γ' solvus temperature of this alloy is about 1470K. Heat-treatment conditions were selected from wide range above and below the γ' solvus temperature. Heat-treated specimens were cut and microstructure observations were conducted by optical microscope. The grain size was measured by linear intercept method.

Results and discussion

Microstructure of as-forged N18 is shown in **Fig.1**. As-forged N18 has a homogeneous microstructure and the grain size of the pancake is about 6μm. The microstructure of N18 consists of the γ, primary γ' with a few microns in size, secondary γ' and tertiary γ' (Wlodek et al., 1992). The primary γ' indicated by an arrow are shown at the grain boundaries.

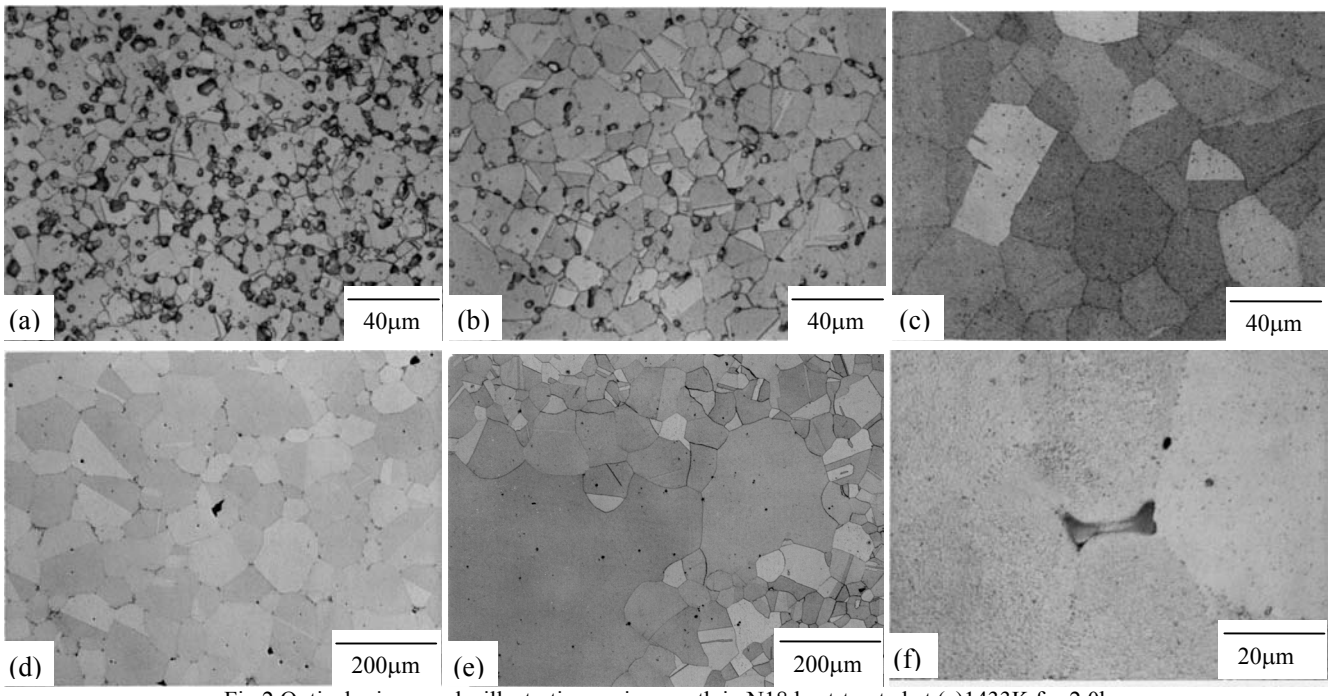

Fig.2 Optical micrographs illustrating grain growth in N18 heat-treated at (a)1433K for 2.0h, (b)1453K for 2.0h, (c)1473K for 2.0h, (d)1493K for 2h and (e)1473K for 8h (f)1493K for 2.0h

Single step solution-treatment. Optical micrographs of heat-treated specimens are shown in **Fig.2**. Volume fraction of the primary γ' decreases and the grain size increases gradually as the temperature increases. (**Fig.2 (a) and (b)**) Then at 1473K the primary γ' was fully dissolved, and the grain size increase drastically up to 1493K. (**Fig.2 (c), (d)**) Grain size seems to be controlled by the dissolve behavior of the primary γ'. However, prolonged heat-treatment at 1473K led to anomalous grain growth as shown in **Fig.2 (e)**. This type of large grain cannot be acceptable from the point of LCF strength. On the other hand, at 1493K some black spots were observed on the grain boundaries. These spots are the incipient melting occurring during heat-treatment (**Fig.2 (f)**). Grain sizes of heat-treated specimens are clearly controlled by solution treatment temperature, however, some problems such as abnormal grain growth and incipient melting have occurred.

Grain growth behavior for 2h heat-treatment is shown as a function of temperature in **Fig.3**. The grain growth behavior is changed at about 1450K. Below the threshold temperature, the grain size almost remains unchanged, but above 1450K the grain size increases drastically.

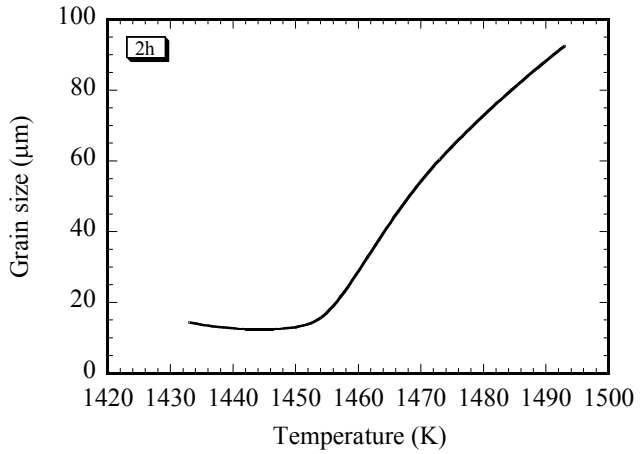

Fig.3 The grain growth behavior heat-treated at various temperature for 2h as a function of heating temperature.

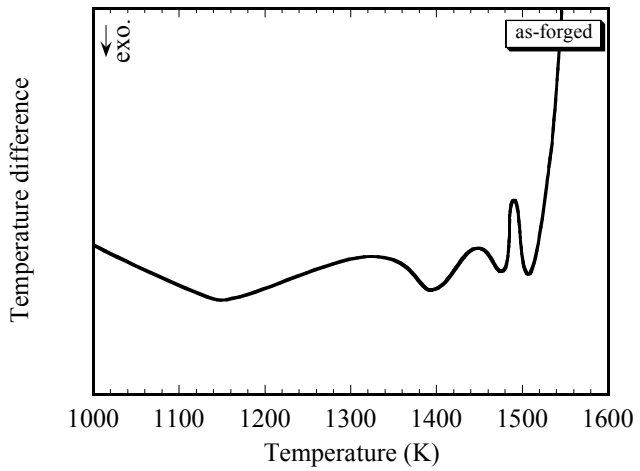

Fig.4 Heating thermogram for as forged N18. Heating rate: 20K/min

Heating thermogram for as-forged N18 is shown in **Fig.4**. The peaks from 1400K to 1470K indicate the dissolution of the primary γ' as shown in **Fig.2**. The threshold temperature, 1450K, is in agreement with the primary γ' dissolved temperature. It is assumed that the primary γ' acts as a resistance of grain growth. Therefore in order to obtain coarse grain size, the primary γ' precipitated on the grain boundaries should be dissolved.

It has reported that two grain growth temperatures are observed in Ni-base P/M superalloy containing high γ' volume fraction by Chang (1996). It is believed that the two temperatures are associated with the γ' solvus temperature and MC carbide solvus temperature. In this study, this behavior was not observed. MC carbide solvus temperature was not observed clearly in terms of microstructure. However, endothermic reaction detected at 1495K might indicate the MC carbide dissolution. In this case, second grain growth temperature by MC carbide dissolution is above testing conditions.

Two steps heat-treatment. In order to avoid the formation of anomalous large grains and incipient melting on the grain boundaries, new two steps heat-treatment condition was tested. The aim of the first step treatment is to decrease the volume fraction of primary γ' acting as resistance for grain growth. In this stage the temperature is below 1473K in terms of inhibition of the incipient melting. As for the second step, aim of this stage is to enhance grain growth without formation of anomalous grain growth. Therefore heat-treatment condition was selected as shown in **Table 2(R1)**.

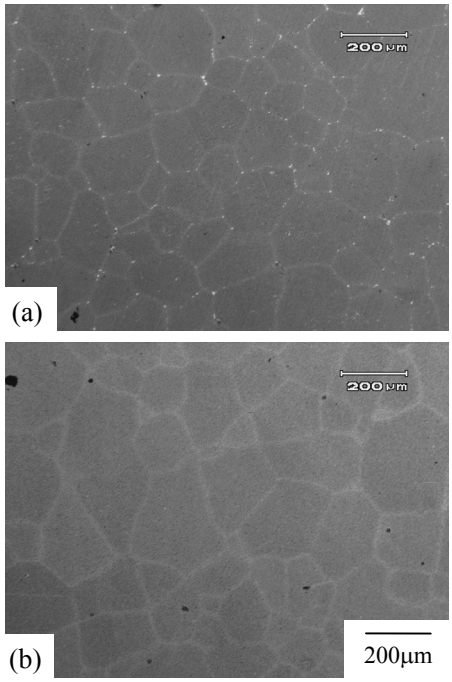

Fig.5 Microstructure of N18 heat-treated at 1453K for (a)1h and (b)2h after 1473K for 0.5h.

Microstructures heat-treated at 1473K for 0.5h followed by 1453K for 1 and 2 h are shown in **Fig.5**. The specimen treated for 1h in second stage has the primary γ' slightly (**Fig.5 (a)**) even though heated at 1473K for 0.5h. As heat treatment time of the second stage increases, the primary γ' are fully dissolved and their grain size increases. As shown in **Fig.5 (b)**, homogeneous and large grains are obtained.

Grain growth behavior is shown as a function of heat-treatment temperature and time in **Fig.6**. The change in grain size treated at 1453K without the first stage treatment is small. The grain size heat-treated for 8h is about 22μm. On the other hand, grain growth behavior of the specimen applied two steps treatment is completely different from that of the directly treated specimen. The grain size after the first stage treatment is about 36μm, and then the grain size

increases gradually. After 4h treatment the grain size becomes about 80μm.

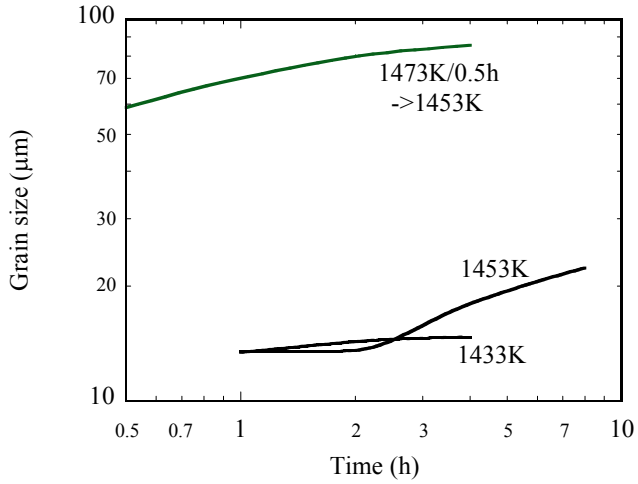

Fig.6 Grain growth behavior of N18 as a function of heat-treatment time.

In order to apply this behavior to microstructure prediction model, the activation energy of the grain growth was estimated.

Prediction of heat-treated microstructure. In general, the grain growth behavior is descried by the Arrhenius type plot using cubic grain size and reciprocal temperature. **Figure 7** shows the relationship between the cubic grain size at 1473K and 1493K for 2h and reciprocal temperature. In this condition, the primary γ' were fully dissolved. From the slope of this curve, the activation energy of grain growth is estimated about 371kJ/mol. This value is smaller than those of other superalloys such as Waspaloy (Shen et al., 1996). Using this value, the grain size of the material using two steps heat treatment is represented by **Eq.(1)**. Additionally **Eq.(2)** is obtained using initial grain size before second step.

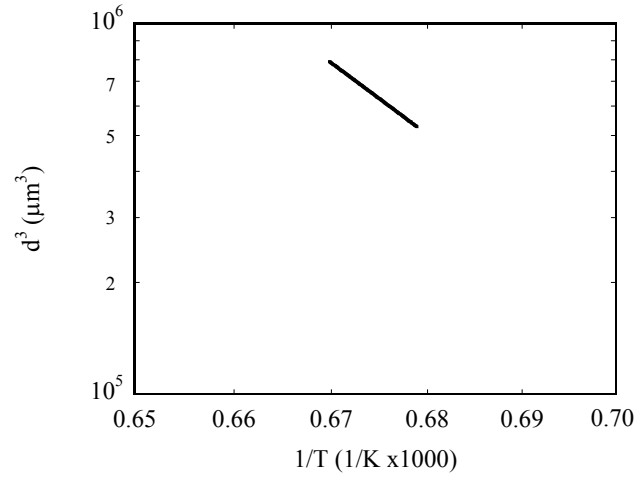

Fig.7 Temperature dependence of the grain growth in as-forged N18.

Grain size distribution after the heat-treatment for dual-property disk was predicted in accordance with **Eq.(2)**. Making process using for prediction model is as follows; firstly the outside of the disk is heated by the induction heating. After cooling, the whole disk is heated in the furnace. The grain size distribution across s the disk is presented in **Fig.8**. The microstructure in the outside of the disk consists of coarse grain, and the size is about 73mm. On the other hand, the grain size is kept under 18 μm inside of the disk.

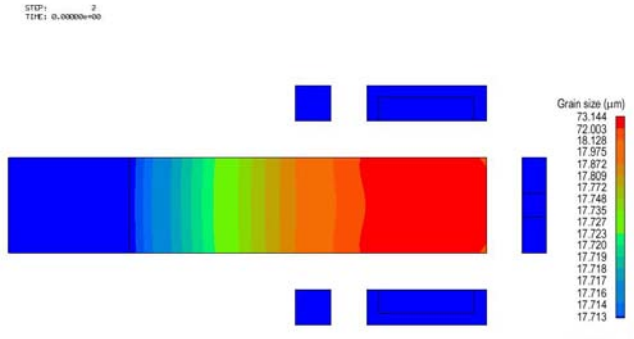

Fig.8 Contour diagram of the cross section of heat-treated disk.

MICROSTRUCTURE PREDICTION

In case of using C&W material, the forging condition strongly affects the microstructure. During forging process, dynamic recrystallization occurs and the grain size changes consequently. Temperature, strain rate and strain are significant conditions for microstructure formation. In order to obtain ideal forging condition, trial productions have been repeated. However, from the view of cost reduction, several trial leads to the rise of the production costs, therefore it should be avoided. According to this situation, various microstructure prediction models have been investigated. In this section, the development of microstructure prediction model is introduced.

Experimental procedure

Experimental material is a billet of C&W U720LI. The chemical composition of material is given in **Table 3**. The ingot of the material was made by triple melting method and it was cogged to 10 inches billet. The grain size of the billet is about 16μm. In order to access the high temperature deformation behavior, ϕ8x10mm specimens were cut from the billet. High temperature compression tests were conducted at the strain rate ranging from 0.03 to 0.1 1/s and the temperature from 1348 to 1433 K. Compression tests were interrupted at the various strain. The specimens were cut parallel to the stress axis. Microstructural observation was conducted using the optical microscope. From the obtained data on grain size and deformation behavior, microstructure prediction model for U720LI was established.

Table 3 Chemical composition of U720LI (wt%)

Cr	Co	Mo	W	Ti	Al	C	B	Zr	Ni
16.0	14.4	3.0	1.2	5.0	2.7	.015	.016	.04	Bal.

Results and discussion

Compression tests. **Figure 9** shows the typical stress strain curves of compression tests of U720LI. Each curve has a large peak at the strain around 0.06-0.1and a small peak in lower strain region. After the large peak, the flow stress decreases and becomes the plateau. The amount of decrease in flow stress becomes small as temperature increase. The strain at the peak stress also increases, as increasing temperature. These results suggest that dynamic recrystallization occurs during deformation. In order to estimate the high temperature deformation behavior, the effect of the temperature on the flow stress was estimated.

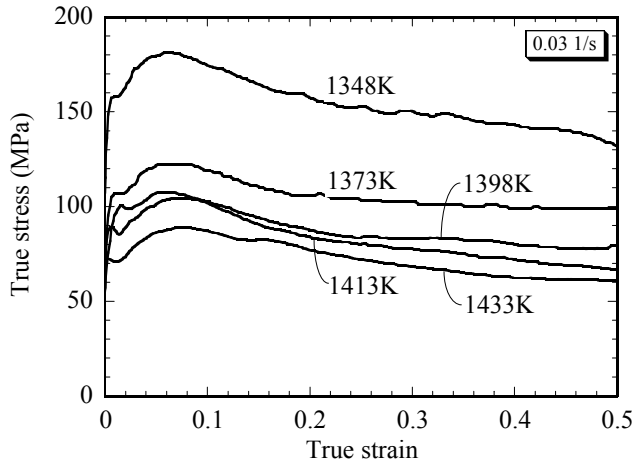

Fig. 9 Typical stress-strain curves in compression tests at various temperature of as-billet U720LI.

The relationship between true strain rate and flow stress is shown in **Fig.10**. The flow stress increases as temperature increases, and a linear relation between them was obtained in log-log plot. The stress exponent n is about 4 in this study.

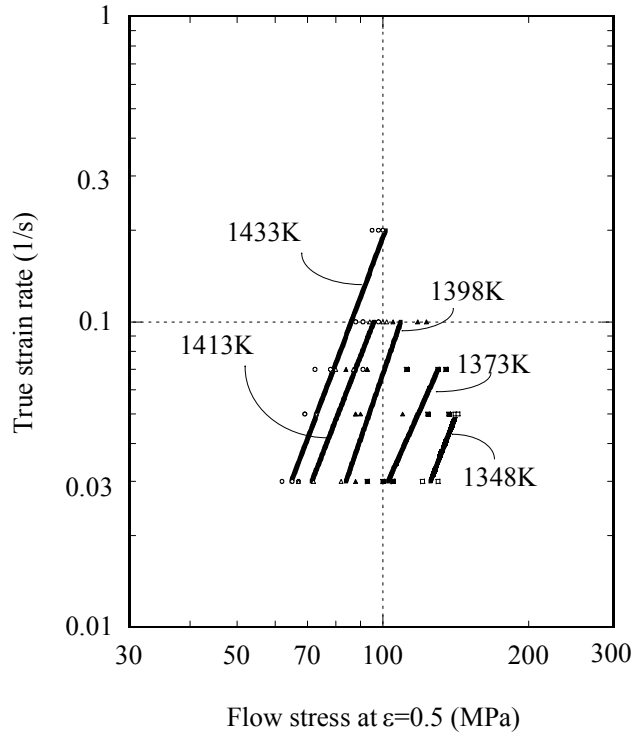

Fig.10 Relationship between flow stress and true strain rate at various temperatures in as-billet U720LI.

In general, the relation between flow stress and strain rate is represented as shown in **Eq.(3)** (Cadek,1988). Activation energy of deformation was estimated using this relation. The ratio of σ^n at the strain 0.5 to true strain rates was plotted as a function of the reciprocal temperature in **Fig.11**. In this figure, stress exponent 4 is applied as a result of **Fig.10**. The slope of the curve is changed at about 1380K that was the pre-heat temperature before the compression tests. Shen et al.(1996) attribute the two line segment to super-solvus and sub-solvus respectively. However, the bend point was not observed at the γ' solvus temperature. From the slope of this line, activation energy for deformation is estimated about 473kJ/mol. This value is higher than that of waspaloy (Shen et al., 1996).

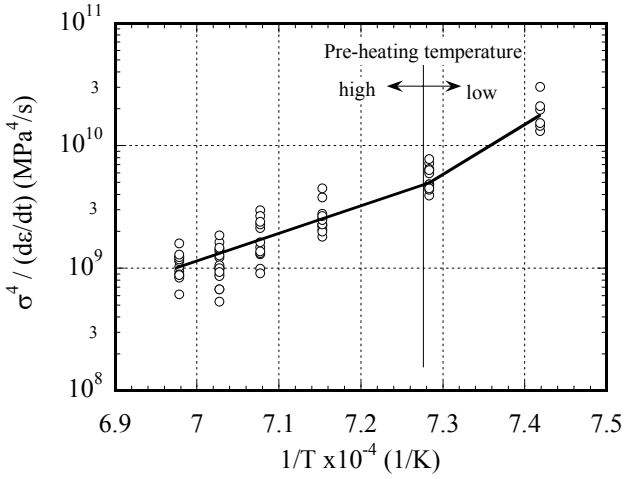

Fig.11 Temperature dependence of $\sigma^4/(d\varepsilon/dt)$ in compression tests of as-forged U720LI.

Prediction of forged microstructure. Dynamically recrystallized grain size was plotted using Zener-Hollomon parameter in **Fig.12**. In order to estimate the obtained dynamic grain size data from the different testing condition, Z parameter that was shown in **Eq.(4)** is used. From these results dynamic recrystallize grain sizes were represented by **Eq.(5)**. Exponent of Z was small compared with the value of waspaloy (Shen et al., 1996). This result also suggests the deformation resistance of U720LI is higher than that of waspaloy.

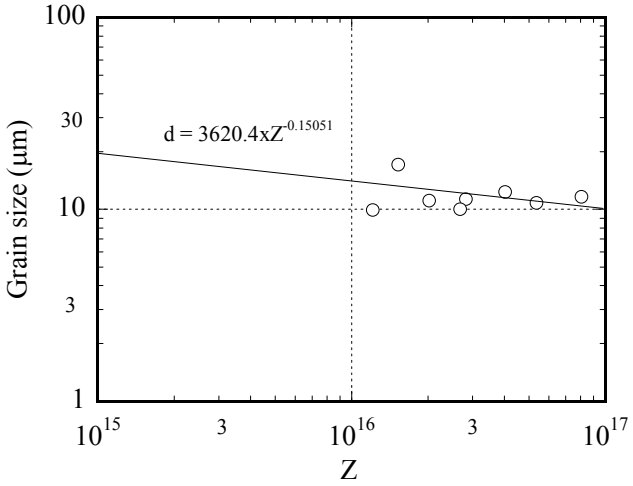

Fig.12 Effects of compression temperature and strain rate on dynamic recrystallized grain size during compression tests in U720LI.

Using above relation between Z parameter and the dynamically recrystallized grain size, grain size distribution was calculated and the accuracy of prediction for grain size was estimated. The relationship between the calculated grain size and experimental grain size are shown in **Fig.13**. In this figure, the grain size was

normalized. The calculated values are qualitatively in agreement with an actual values. The accuracy of prediction is within +-5%.

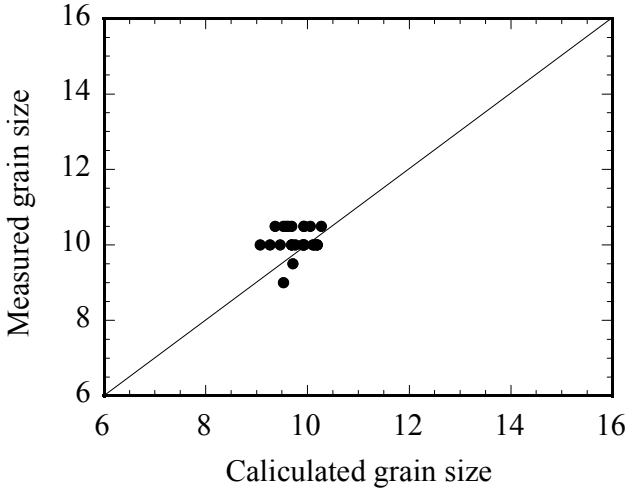

Fig.13 Comparison between the calculated and measured grain size in U720LI.

MECHANICAL PROPERTIES PREDICTION

Metallurgical problems, such as grain size variation and inhomogeneity of the precipitation, may occur when the ingot size is scaled up (Helms, 1996). It is difficult to eliminate the inhomogeneous structure by forging and heat treatment process. The developed prediction system cannot predict the mechanical properties of material that has an inhomogeneous structure. Limited information including mechanical properties is reported regarding the inhomogeneity due to solidification segregation.

U720LI billet that is made from a large ingot has a band structure. There are two features of the band structure, i.e. the primary γ' distribution and the grain size. In this work, we have considered the effects of the inhomogeneity, precipitation band and local grain size variation, on mechanical properties of cast/wrought U720LI. On the basis of these experimental results, positive modification in prediction model is also discussed.

Experimental procedure

Experimental material is cast/wrought U720LI that is the same as the material using in the previous section. Pancake forgings were conducted using the sample cut off from the billet at three different temperatures, T1, T2 and T3 (see **Table 4**). The forged pancakes were solution treated at 1378K/2h/O.Q. and aged at 922K/24h/G.F.C. and 1033K/8h/G.F.C.. Grain sizes of heat-treated specimens were measured by intercept method.

In order to assess the effect of inhomogeneous microstructural features on mechanical properties, various mechanical tests were conducted. Creep and LCF specimens were machined from heat-treated pancakes. A gage length and diameter of the creep specimen was 30mm and 6mm respectively. Creep tests were carried out at 973, 1033 and 1073K at the stress range of 350-620MPa. LCF specimens had a gage length of 25mm with 6mm in diameter. Axial strain control LCF tests were performed using 30cpm triangle wave and strain A ratio of 1.0 at 673K, in the strain range 0.8-1.6%.

Results and discussion

Microstructural feature of the billet is shown in **Fig.14**. Bands that are extended to longitudinal direction are observed. Widths of the bands are about 100-200μm. In this figure, black particles are primary γ' precipitates. The bands consist of alteration of fine primary γ' precipitated area and the coarse primary γ' precipitated area. Grain size is also different due to primary γ' precipitated morphology.

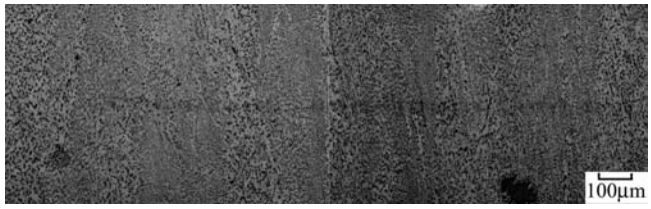

Fig.14 Microstructure of the U720LI billet. Longitudinal direction is vertical.

Table 4 Grain size of forged pancakes (μm)

	Fine grain area	Coarse grain area	Average
T1	5.5	10.0	7.8
T2	7.4	11.0	9.2
T3	8.5	22.3	15.4

With increase in forging temperature, the volume fraction of primary γ' decreases, however, T3 forged at supersolvus temperature still has primary γ' precipitates. The solvus temperature of the primary γ' is above the forging and the heat-treatment temperature therefore the band structure was not broken down (Jackson et al., 1999). Grain sizes of these specimens are shown in **Table 4**. In the fine grain region, the grain size of T3 is 1.5 times larger than that of T1, however, in the coarse grain region, the grain size of T3 is 2.2 times larger than that of T1. The forging temperature influences on coarse grain area more than fine grain area.

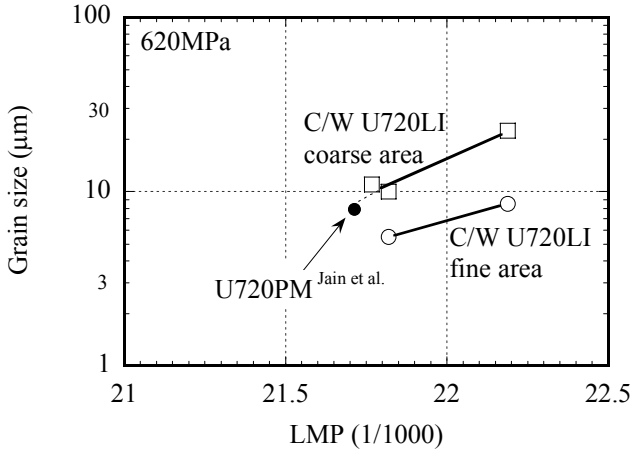

Fig.15 Relationship between grain size of as-heat treated U720LI and creep life on 620MPa at various temperature. The data of U720PM is from Jain et al.

The effects of the coarse and fine grain on the mechanical properties are estimated. The relationship between creep rupture live and grain size is shown in **Fig.15**. In this figure both the coarse and fine grain size are plotted. Creep data of P/M U720 reported by S.K. Jain et al. (2000) are interpolated and plotted in the same figure. Creep lives in this study is represented well by using either fine grain size or coarse grain size respectively, however, creep data of PM U720 that has homogeneous grain size is good agreement

with the data of coarse grain size of this study. This fact suggests that creep rupture lives are governed by coarse grain size.

Similar estimation was also conducted for LCF strength. The relationship between the number of failure of T1, T2 and T3 at 673K and the grain sizes is shown in **Fig.16**. The data of PM U720 reported by S.K. Jain et al. (2000) is also shown. As the relationship between the fine grain size and Nf, the grain size becomes fine, Nf increases linearly in log-log plot. However, the shape of the curve of the coarse grain size is different from that of fine grain size. As the grain size decreases from 22 to 12μm, as, Nf increases gradually, but bellow 12μm, the slope of curve becomes shallow and sensitivity to grain size is depressed.

The data of PM U720 is close to the curve of the coarse grain size when the coarse grain size is above 12μm. On the other hand, it is close to the curve presented by the fine grain size when the coarse grain size is below 12μm. This fact suggests that the effects of the coarse grain on LCF lifetime disappear below the threshold grain size of 12μm. The detail of this behavior is under investigation.

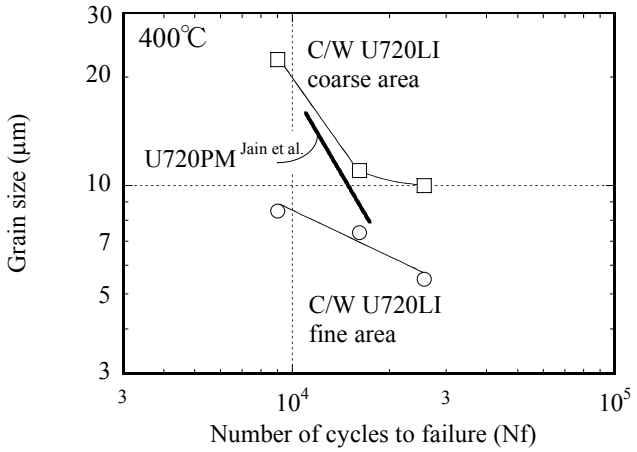

Fig.16 Relationship between grain size of as-heat treated U720LI and number of cycles to failure. LCF tests were conducted at 400C and total strain was at the range from 0.8 to 1.6%. The data of U720PM is from Jain et al.

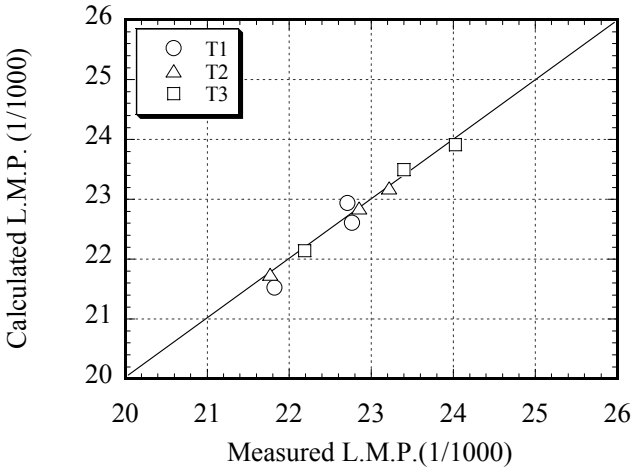

Fig.17 Comparison between calculated and measured creep life for U720LI.

The equations for the prediction of creep lives and LCF lifetime are made. In case of using average grain size, the accuracy of prediction is not good. In this study, specific grain size that strongly affects mechanical properties is applied based on the above investigation.

The equation for creep life prediction is made as follows; all of the creep rupture data are converted to the lives at 923K using Larson-Miller parameter and presented as a function of the applied stress. Then constant term and stress exponent are approximated as a function of the coarse grain size. Obtained equation showing the relation between the coarse grain size and the creep life at 923K is shown in **Eq.(6)**. The result of the prediction is shown in **Fig.17**.

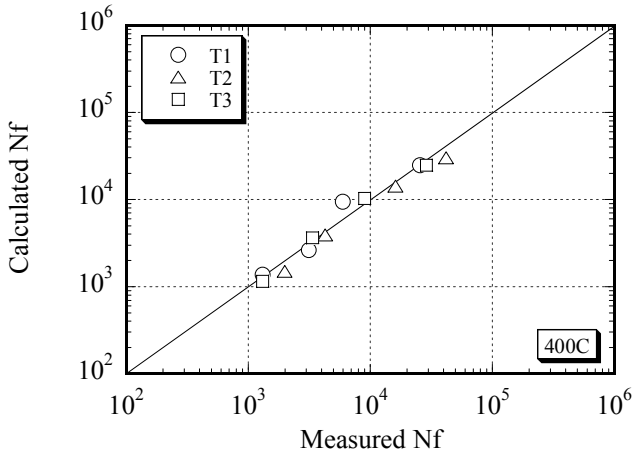

Fig.18 Comparison between calculated and measured LCF life for U720LI

LCF strength is estimated as follows; all of measured Nf data of T1, T2 and T3 at 673K was presented as a function of total strain range respectively. Then constant term and exponent of strain range were approximated as a function of the grain size. Obtained equations are given in **Eq.(7)** and **Eq.(8)**. Based on the previous estimations, the applicable equation depends on the coarse grain size. When the coarse grain size is larger than 12μm, **Eq.(7)** is applicable using the coarse grain size. On the other hand when the coarse grain size becomes smaller than 12μm, some coefficients are different. Then, the equation shown in **Eq.(8)** is applied for the fine grain size as a grain size in this equation. Prediction results are shown in **Fig.18**. Calculated data are good agreement with the measured data.

SUMMARY

In this paper, overview of the turbine disk development was introduced in terms of dual-property disk production and mechanical property prediction. The conclusions can be summarized as follows;

1. Grain growth behavior was controlled by primary γ' precipitation by pinning of grain boundaries. Above 1473K primary γ' is dissolved, therefore grain size increases rapidly. However, prolonged heat-treatment at 1473K led to anomalous grain growth and above 1493K incipient melting occurred.
2. Two steps heat-treatment, i.e. 1473K/0.5h and 1453K, leads to homogeneous and coarse microstructure without incipient melting.
3. From the above investigation, grain size distribution of the disk was calculated.
4. The forged and heat-treated specimen has a band structure consisting of the fine and the coarse grain region.
5. Creep rupture lives in this study are affected by the grain size of the coarse grain region.
6. Influence of the inhomogeneous microstructure on LCF strength of U720LI was affected the coarse grain size. When the grain size is

larger than 12μm, LCF strength can be calculated using the coarse grain size. On the other hand, the strength can be calculated by the fine grain size when the grain size is smaller than 12μm.
7. Calculation model for the mechanical property prediction was made on the basis of inhomogeneous structure. The predicted properties were in good agreement with the measured values.

Equations

$$d^3 = 7.50\times10^{18}\cdot\exp\left(-\frac{370888}{RT}\right) \quad (1)$$

R: gas constant
T: heat-treatment temperature (K)

$$d^3 = {d_0}^3 + 1.23\times10^{18}\cdot t\cdot\exp\left(-\frac{370888}{RT}\right) \quad (2)$$

R: gas constant
T: heat-treatment temperature (K)
t: heat-treatment time (h)
d_0: initial grain size (μm)

$$\frac{d\varepsilon}{dt} = C\cdot\exp\left(-\frac{Q}{RT}\right)\cdot\sigma^n \quad (3)$$

ε: strain
σ: flow stress
Q: activation energy
R: gas constant
T: temperature
C: constant

$$Z = \frac{d\varepsilon}{dt}\cdot\exp\left(\frac{Q_{df}}{RT}\right) \quad (4)$$

ε: strain
Z: Zener-Hollomon parameter
Q_{df}: The activation energy of deformation
T: Temperature
R: Gas constant

$$d_{dyn} = 3620.4\times Z^{-0.15} \quad (5)$$

d_{dyn}: dynamic recrstallized grain size (μm)
Z: Zener-Hollomon parameter

$$t_r = 1.06\times10^6\cdot d^{14.5}\cdot\sigma^{-(4.9+0.13\cdot d)} \quad (6)$$

t_r: creep life (h)
d: coarse grain size (μm)
σ: applied stress (MPa)

$$N_f = 1.68\times10^5\cdot d^{-0.91}\cdot d^{-7.67\cdot d^{-0.16}} \quad (7)$$

Nf: number of cycles to failure
d: grain size (μm)
ε_t: total strain range (%)

$$N_f = 3.83\times10^5\cdot d^{-1.64}\cdot\varepsilon_t^{-9.8\cdot d^{-0.34}} \quad (8)$$

Nf: number of cycles to failure
d: grain size (μm)
ε_t: total strain range (%)

Acknowledgement

The authors would like to express their thanks to the New Energy and Industrial Technology Development Organization (NEDO) and the Ministry of Economy, Trade and Industry (METI), who gave them the opportunity to conduct "Research and Development of Environmentally Compatible Propulsion System for Next-Generation Supersonic Transport (ESPR) project".

References

J.M. Hyzak, C.A. Macintyre, D.V. Sundberg, 1988, "Dual Structure Turbine Disks Via Partial Immersion Heat Treatment", Superalloys 1988 (Warrendale, PA; The Minerals, Metals and Material Society), pp.121-130

G.Shen, J.Rollins, D.Furrer, 1996, "Microstructure Modeling of Forged Waspaloy Disks", Superalloys 1996 (Warrendale, PA; The Minerals, Metals and Material Society), pp.613-620

J. Cadek, 1988, " Creep in Metallic Materials", Elsevier Science Ltd., p.p.44-59

M. Chang, A.K.Koul, C.Cooper, 1996, "Damage Tolerance of P/M Turbine Disk Materials", Superalloys 1996 (Warrendale, PA; The Minerals, Metals and Material Society), pp.667-685

A.D. Helms, C.B. Adasczik, L.A. Jackman, 1996, "Extending the Size Limits of Cast/Wrought Superalloy Ingots", Superalloys 1996 (Warrendale, PA; The Minerals, Metals and Material Society), pp.427-433

M.P. Jackson, R.C. Reed, 1999, "Heat Treatment of UDIMET 720Li: The Effect of Microstructure on Properties". Mater, Sci. Eng., A259, pp.85-97

S.K. Jain, B.A. Ewing and C.A. Yin, "The Development of Improved Performance PM UDIMET 720 Turbine Disks", Superalloys 2000 (Warrendale, PA; The Minerals, Metals and Material Society), pp.785-794

S. Takahashi, S. Nishikiori, T. Iwasaki, T. Tanaka, 2001, "Effects of forging temperature on mechanical properties" Microstructure Modeling and Prediction During Thermomechanical Processing (Warrendale, PA; The Minerals, Metals and Material Society), p.p.167-173

S.T. Wlodek, M. Kelly, D. Alden, 1992, "The Structure of N18", Superalloys 1992 (Warrendale, PA; The Minerals, Metals and Material Society), pp.467-476